


Boronate affinity-mediated magnetic solid phase extraction and bioactivities of polysaccharides from beverage plants

Yuwen Ding^{1#}, Haiyang Li^{1#}, Tao Liu¹, Yan Liu², Minghan Yan¹, Liangjingjing Shan¹, Xiaomeng Liu¹, Tingxuan Yan¹ and Shuangshou Wang^{1,3*} 

¹ School of Chemistry and Chemical Engineering, Anhui University of Technology, Maanshan 243032, China

² Maanshan Institute for Food and Drug Control and Adverse Drug Reaction, Maanshan 243000, China

³ Anhui Engineering Technology Research Center of Biochemical Pharmaceutical, Bengbu Medical College, Bengbu 233030, China

These authors contributed equally: Yuwen Ding, Haiyang Li

* Corresponding author, E-mail: wangss17@ahut.edu.cn

Abstract

Polysaccharides are of great significance in food production, but their isolation highly relies on multi-staged liquid-liquid extraction. In this study, a boronate affinity-mediated magnetic solid phase extraction (BA-MSPE) method was initiated for the effortless and efficient extraction of polysaccharides using boronic acid-grafted magnetic nanospheres (MNPs@B(OH)₂) as extractants. MNPs@B(OH)₂ showed fine class selectivity toward *cis*-diol containing compounds at weak alkaline condition (pH 7.5~8.5) and higher binding capacity than that of MNPs without boronic acid functionalization. Fast binding dynamics with a binding equilibrium within 10 min, stronger affinity toward polysaccharides (K_d as low as 10^{-3} ~ 10^{-6} M level) than that of small molecular *cis*-diol compounds (K_d in the range of 10^{-1} ~ 10^{-4} M level), and good recyclability (the binding capacity decreased less than 13% after ten times consecutive extraction) could also be observed for MNPs@B(OH)₂. Finally, the BA-MSPE of polysaccharides was performed with three beverage plants as real samples, including tea leaves, soybeans, and *Lycium barbarum*. Antioxidant activity of polysaccharide extractives was verified by DPPH radical scavenging assays, giving a radical scavenging rate of 31.4% and 18.8% for crude extractives of TPS (tea polysaccharide) and LBPS (*Lycium barbarum* polysaccharide), respectively. Microscopic imaging combining with MTT and trypan blue staining trials uncovered that the extractives were of dosage-dependent antitumor bioactivities, giving the cell mortality rates over 91.8% and 77.2% for MCF-7 and A549 cells in the presence of 5.0 mg/mL TPS, and 56.6% and 40.0% with the equal dosage of LBPS, respectively. As the BA-MSPE strategy is simple and eco-friendly, there will be more potential for the application of *cis*-diol compound purification.

Citation: Ding Y, Li H, Liu T, Liu Y, Yan M, et al. 2023. Boronate affinity-mediated magnetic solid phase extraction and bioactivities of polysaccharides from beverage plants. *Beverage Plant Research* 3:14 <https://doi.org/10.48130/BPR-2023-0014>

Introduction

Polysaccharides are heavily used in foods, cosmetics and preventive medicines due to their various bioactivities and low side effects^[1]. To purify polysaccharides with high yield, a high number of strategies have been reported^[2,3], including size exclusion chromatography, ultrafiltration, dialysis, water extraction combined with ethanol precipitation, machine-assisted extraction, and enzymolysis approaches, etc. In spite of this, time-consuming separation and impurity removal steps are often essential for these methods. Simple and efficient strategies for polysaccharide extraction are still scarce, but highly desired.

Magnetic solid phase extraction (MSPE) has been proven to be a powerful tool for separation and purification related applications^[4-6], in which the magnetic nanoparticles are applied as sorbents, then the extraction and elution processes can be easily completed by external magnetic field while, without extra instrument-assisted separation operations such as centrifugation and ultrafiltration, and high pressure required in traditional SPE column or cartridge can also be avoided. Large specific surface area of magnetic nanospheres (MNPs) enables MSPE to obtain high extraction capacity, and the vast majority of MNPs can be easily recycled by external magnets. As a result,

the operations for separation can be significantly simplified, the extraction efficiency can be improved, and the cost can be also reduced. Admittedly, MSPE provides a promising pathway for polysaccharide purification, but such an idea is still in its infancy.

Boronate affinity effect^[7-9] is a reversible covalent binding between 1,2- and 1,3-*cis*-diol containing compounds and boronic acid moieties, of which the covalent five- or six-membered cyclic boronate ester can be formed at a basic pH condition while the bound *cis*-diol compounds can be reversibly released when the system pH changes to acidic. Thanks to such a unique pH-adjustable binding, boronate affinity effect has been widely used for affinity separation^[10] and chemical sensing^[11] of *cis*-diol compounds. Under such a background, a boronate affinity-mediated MSPE (BA-MSPE) strategy was pioneered herein for the easy isolation of polysaccharides. The schematic for this protocol is illustrated in Fig. 1 using the possible structure of tea polysaccharide (TPS) as a representative^[12], in which boronic acid-functionalized MNPs were served as sorbents. Because the abundant 1,2- and 1,3-*cis*-diol structures in backbone and/or branch carbohydrate chains were their universal hallmarks, polysaccharides would be extracted under weak

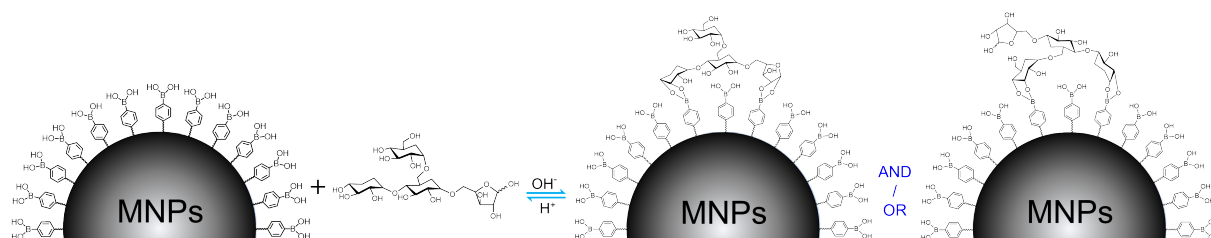


Fig. 1 The general binding mechanism for polysaccharide extraction by boronic acid-decorated MNPs using possible chemical structure of TPS as a representative.

alkaline condition by multisite binding-based positive synergistic boronate affinity effect, and then the extractives could be reversibly released after altering the system pH to acidic. By such a simple process, three polysaccharides, including TPS, *Lycium barbarum* polysaccharide (LBPS) and soybean polysaccharide (SPS), were effectively isolated from relevant real beverage plants, and their antioxidant and antitumor bioactivities were also demonstrated.

Materials and methods

Chemicals and plant materials

Acetic acid (HAc, 99.5%), KH_2PO_4 (99.5%), NaH_2PO_4 (99.9%), Na_3PO_4 , H_3PO_4 , NaOH, chloroform ($\geq 99\%$) and $\text{FeCl}_3 \cdot 6\text{H}_2\text{O}$ (99%) were purchased from Sinopharm Chemical Reagent Co., Ltd. (Shanghai, China). Ethylene glycol ($> 99\%$), sulfuric acid (96%), 3-methyl-1-phenyl-2-pyrazoline-5-one (PMP, 99%), 4-formylphenylboronic acid (FPBA, 98%), methanol (99.5%), 1,6-hexamethylenediamine (99%) and anhydrous sodium acetate (99.5%) were purchased from Titan Scientific Co., Ltd. (Shanghai, China). 2,2-Diphenyl-1-picrylhydrazyl (DPPH, 98.5%), thiazolyl blue tetrazolium bromide (MTT, $> 99\%$), HPLC-grade acetonitrile (ACN), trifluoroacetic acid (TFA, 99%), anhydrous ethanol and phenol were obtained from Macklin Biochemical Co., Ltd. (Shanghai, China). Pullulan polysaccharide (PPS, 99%), tea polysaccharide (TPS, 50%), soybean polysaccharide (SPS, 70%), *Lycium barbarum* polysaccharide (LBPS, $\geq 50\%$), trypan blue (60%) and deoxyguanosine (99%) were from Yuanye Bio-Technology (Shanghai, China). NaBH_3CN (95%), guanosine (99%), adenosine (99%), deoxyadenosine (99%) and cytidine (99%) were from Aladdin Bio-Chem Technology Co., Ltd. (Shanghai, China). Human breast cancer cell line (MCF-7), human lung carcinoma cell line (A549), Roswell Park Memorial Institute 1640 medium (RPMI-1640, containing 2.0 mg/mL D-glucose, 0.3 mg/mL glutamine, 2.0 mg/mL NaHCO_3 , 80 U/mL penicillin, and 0.08 mg/mL streptomycin), Dulbecco's Modified Eagle Medium (DMEM, containing 4.5 mg/mL D-glucose, 0.3 mg/mL glutamine, 0.11 mg/mL sodium pyruvate, and penicillin streptomycin), penzyme cell digestion solution (containing 0.25% trypsin and 0.02% EDTA), and phosphate buffer solution for cell culture (PBS) were purchased from Keygen Biotech (Nanjing, China). Fetal bovine serum (FBS) was purchased from Gibco (Life Technologies, Australia). Cell culture bottles (25 cm^2 in growth area) and glass bottom cell culture dishes (Φ 30 mm) used for cell culture and microimaging were obtained from NEST Biotechnology (Wuxi, China). Real-world beverage plants, including *Lycium barbarum*, tea leaves (green tea) and soybeans, were purchased from a local supermarket. Water used in this study was produced by a Milli-Q system (Millipore, Milford, MA, USA). Except as otherwise noted, the purity grades

of all chemicals without specific stipulations were analytically pure and phosphate buffer (PB) solutions used in this work was especially referred to the 0.1 M, pH 8.5 phosphate buffer.

Synthesis of MNPs@B(OH)_2

MNPs@B(OH)_2 were prepared referring to our previous reports^[4,5] with slight modifications, in which the preparation of amino group-capped MNPs (bare MNPs) and then their post-modification with FPBA were contained. To synthesize bare MNPs, 480 mL ethylene glycol, 16.0 g FeCl_3 and 32.0 g anhydrous sodium acetate were mixed, then the mixture was slowly heated to 55 °C and kept vigorously stirring until the solution became transparent, followed by adding with 104.0 g 1,6-hexamethylenediamine and mixing evenly. After that, the resulting solution was transferred into a polytetra-fluoroethylene autoclave reactor and kept under reaction for 10 h at 198 °C. Finally, the prepared bare MNPs were magnetically separated and washed three times with ethanol and water, then the obtained MNPs were dried in a vacuum oven at 55 °C and stored in an air tight container.

For the boronic acid functionalization, 2.0 g the above prepared MNPs were dispersed into 100 mL absolute ethanol containing 5.0 mg/mL FPBA and 1.0 mg/mL NaBH_3CN . After ultrasound for 30 min, the mixed solution was mechanically agitated at 40 °C for 12 h. When the reaction finished, the MNPs@B(OH)_2 were magnetically isolated and respectively rinsed three times with ethanol and water, and then harvested after drying at 55 °C and stored under air tight conditions for upcoming assays.

Binding selectivity and adsorption dynamics of BA-MSPE

Deoxyguanosine, deoxyadenosine, cytidine, guanosine and adenosine were served as model compounds to investigate the binding selectivity of MNPs@B(OH)_2 . Briefly, 8 mL aliquots of PB containing 1.0 mg/mL model analytes were supplemented with 35.0 mg MNPs@B(OH)_2 or bare MNPs, after fully dispersing by ultrasonic, the resulting mixture solutions were incubated at room temperature for 0.5 h. Then the analyte-extracted MNPs@B(OH)_2 or bare MNPs were magnetically separated and redispersed into 1.0 mL desorption solution composed by 0.1 M acetic acid. After desorption for 2 h, the materials were removed by external magnet while the supernatants were collected individually, and their UV-vis absorption spectra were tested on a UV-1800PC spectrophotometer (Mapada Instruments, Shanghai, China). The equilibrium binding capacity of MNPs@B(OH)_2 and bare MNPs was figured out with standard curve method, which measured by UV-vis spectrometry and plotted by licensed OriginPro 2016 software. The wavelengths used for plotting standard curves of adenosine, guanosine, cytidine, deoxyadenosine and deoxyguanosine were, respectively, set at 258, 252, 278, 258 and 258 nm.

Extraction and bioactivities of polysaccharides

For the investigation of adsorption dynamics, guanosine, a *cis*-diol containing compound which can form boronate affinity effect with $\text{MNP}@B(\text{OH})_2$, was selected as a target analyte. The steps were as follows: 35.0 mg $\text{MNP}@B(\text{OH})_2$ was fully dispersed into 5 mL PB containing 0.1 mg/mL guanosine by vortex and ultrasonic. After incubation at room temperature for the appropriate time (0, 5, 10, 15, 20, 30 and 50 min), 200 μL aliquots of this mixture solution were taken out and the supernatants were individually collected after discarding the materials by external magnetic field. Finally, the absorbance of supernatants was measured on a spectrophotometer. The binding dynamics were plotted according to the relationship between the absorbance of supernatants and extraction time.

Influence of pH on BA-MSPE

To probe the effect of pH on the extraction performance of $\text{MNP}@B(\text{OH})_2$, the main operations were the same as above except that the consumption of $\text{MNP}@B(\text{OH})_2$ was 10 mg and the solvents used for the preparation of guanosine solutions were replaced by PB with pH ranging from 2.5 to 12.5 with intervals of one pH unit. The absorbance of desorption solutions was tested and the extraction amounts of $\text{MNP}@B(\text{OH})_2$ at binding equilibrium were calculated using the standard curve method. This assay was repeated in triplicate and the data were averaged for plotting. The relationship between equilibrium extraction amounts and system pH was applied to assess the impact of pH on BA-MSPE.

Adsorption isotherms and the comparison of extraction performance between bare MNPs and $\text{MNP}@B(\text{OH})_2$

Since the direct spectrometric measurement of polysaccharides was difficult due to their poor UV-vis light absorption properties, color development by phenol-sulfuric acid method was utilized for spectral tests of polysaccharides. With the help of phenol-sulfuric acid chromogenic reaction, standard curves of polysaccharides were tested by UV-vis spectrometry as follows: polysaccharide stock solutions with certain concentration gradients (0.75, 0.5, 0.25, 0.1, 0.05 and 0.005 mg/mL for TPS; 1.0, 0.75, 0.5, 0.25, 0.1, 0.05 and 0.01 mg/mL for PPS; 0.5, 0.4, 0.3, 0.2, 0.1 and 0.075 mg/mL for LBPS; 1.0, 0.75, 0.5, 0.25, 0.1, 0.05 and 0.01 mg/mL for SPS) were prepared at first using 0.1 M HAc aqueous solutions as solvents, then phenol solution (5%, wt%), sulfuric acid and the prepared polysaccharide solutions were mixed in volume ratio of 1:5:1, followed by incubating at 55 °C for 10 min. Thereafter, the digital photos of all solutions were recorded using a smartphone (Vivo X80, Guangdong, China) and their UV-vis spectra were determined on a UV-vis spectrophotometer. Standard curves were plotted by absorbance at 488 nm against polysaccharide concentrations, and the extraction amounts of polysaccharides by MNPs and $\text{MNP}@B(\text{OH})_2$ were inferred from linear regression equations for quantitative comparison. All data were obtained by three tests in parallel for quantifications.

Regarding adsorption isotherms, the details were as follows: A series of TPS stock solutions with a concentration gradient of 0.05, 0.1, 0.5, 1.0, 2.0, 4.0, 6.0, 10.0, 20.0 and 50.0 mg/mL were prepared using PB as solvents, then to each an aliquot of 40.0 mg $\text{MNP}@B(\text{OH})_2$ was added, followed by incubation for 2 h at room temperature. After removing the solvents by magnetic separation, the resulting materials were washed three times

with PB, and then supplemented with 1.0 mL aliquots of desorption solution composed of 0.1 M HAc aqueous solutions. After desorption for 2 h, the supernatants were collected *via* magnetic isolation and their absorbance was measured after color development by phenol-sulfuric acid method. The binding isotherms were obtained through the extraction amounts deduced by the absorbance at 488 nm plotting against TPS concentrations. The Hill equation given below was applied to fit data and estimate the binding properties of $\text{MNP}@B(\text{OH})_2$.

$$y = Q_{\max} \cdot x_n / (x_n + K_d^n)$$

Herein, n was the Hill slope while Q_{\max} and K_d were, respectively, the maximum binding capacity and dissociation constant.

As for the dosage-dependent extraction experiments, the main operations were the same as above except that the dosages of $\text{MNP}@B(\text{OH})_2$ were set as 5, 10, 25, 50, 75, 100 and 150 mg using TPS and LBPS as model analytes both with a concentration of 1.0 mg/mL (dissolved in PB).

Extraction of polysaccharides from real-world beverage plants

Three beverage plants, including tea leaves (green tea), soybeans, and *Lycium barbarum*, were devoted as real samples to extract polysaccharides. Three steps, i.e., the pretreatments of raw materials, the preparation of leaching liquors of crude polysaccharides, and subsequent BA-MSPE, were contained in this experiment.

For the pretreatments of raw materials, the above-mentioned three beverage plants were washed with water several times to remove impurities, followed by drying to a constant weight at 55 °C in an electric oven. Then the powders of raw materials were obtained by quickly crushing in a high speed pulverizer.

To prepare the leaching liquors of crude polysaccharides, the above obtained raw material powders were immersed into PB with a material-to-liquid ratio of 1:50 (1.0 g powder per 50 mL PB). After incubation for 2 h at 60 °C, the leaching liquors and solid matters were centrifugally separated (5000 rpm for 10 min) and individually collected, then the solids were immersed into PB again with the same feed ratio and incubation for another 2 h at 80 °C. After further centrifugal separation, the supernatants were collected and gathered with the filtrates of the previous separation. The total leaching liquors were centrifuged again (10,000 rpm for 5 min) and stored at 4 °C after discarding the precipitation.

BA-MSPE were carried out as follows: 4.0 mL aliquots of freshly prepared leaching liquors were respectively added with 100 mg MNPs or $\text{MNP}@B(\text{OH})_2$, followed by incubating for 0.5 h at room temperature. After magnetic separation, the supernatants were removed and 0.1 M HAc aqueous solutions was supplemented into the polysaccharides-extracted materials with 1.0 mL for each. After desorption for 2 h, the desorption solutions were magnetically collected. After color development with phenol-sulfuric acid method, the UV-vis spectra were measured and their colors were simultaneously recorded. The desorption operations were repeated several times until the color of chromogenic solution was indistinguishable by naked eye. The extraction amounts were figured out and weighted according to standard curve method using the absorbance at 488 nm.

Relative purities of polysaccharide extractives analyzed by UV-vis spectrophotometry

In order to survey the relative purities of polysaccharides extracted by MNPs@B(OH)₂, the extractives from tea leaves and *Lycium barbarum* were freeze dried and corresponding standard polysaccharides were devoted as controls in this assay. The main steps for the BA-MSPE of TPS and LBPS were the same as above except that the dosages of leaching liquors and materials were enlarged. In detail, the volume of leaching liquors was set as 400 mL and the usage of MNPs@B(OH)₂ was 2.0 g. Concentrations of extracted and standard polysaccharide samples for absorbance tests were set at 1.0 and 0.5 mg/mL, respectively. The relative purities of polysaccharides extracts were calculated by dividing the amount of polysaccharides obtained from extracts into that of standard polysaccharides.

HPLC analysis

Freeze-dried extracts of TPS and LBPS are denoted as model polysaccharides herein. Due to their poor light-absorbing properties, PMP-based pre-column derivatizations^[13,14] of polysaccharides were essential for HPLC analysis. In detail, 100 µL methanol solution containing 0.5 M PMP was added with equal volume of 0.5 mg/mL polysaccharide solutions, followed by incubation at 70 °C for 2 h. When the labelling reaction was finished, 1.0 mL chloroform was added into the solution, then vortex for 1 min to extract the unreacted PMP reagents. After centrifuging for 1 min at 1000 rpm, the remaining PMP in the bottom layer was removed. Such a PMP separation operation was repeated three times and the resulting PMP-tagged polysaccharides were loaded for HPLC analysis. The standard polysaccharides labelled in the same way were used as benchmarks for qualitative identification and the determinations of HPLC standard curves.

TFA-based hydrolysis was performed to identify the monosaccharide composites of polysaccharides by HPLC, and the details were as follows: polysaccharides were separately dissolved into 2.0 M TFA solution with a final concentration of 10.0 mg/mL, and then reacted in air tight conditions for 6 h at 105 °C. When the reaction completed, the supernatants were centrifugally collected and their pH was adjusted to neutral using 1.0 M NaOH solution. Subsequently, the PMP labelling of hydrolysates and standard monosaccharides was implemented as above. The resulting solutions were finally stored at 4 °C for use.

HPLC conditions were selected referring to an existing method^[15]: A Adams C18-Classic column (SepaChrom S.R.L., 5 µm, 250 mm × 4.6 mm) was equipped for chromatographic separations; The mobile phase was composed by acetonitrile (A) and monopotassium phosphate aqueous solution with pH 6.8 (B) in an isocratic mode with 20% A; Injection volume was set as 20 µL; A pre-equilibration period of 30~60 min was applied between two consecutive separations; The flow rate and column temperature were, respectively, set as 1.0 mL/min and 40 °C, and the wavelength of 248 nm was selected for detection. All buffer and sample solutions were filtrated using a 0.45 µm filter membrane before running.

HPLC standard curves were plotted in terms of the function between peak areas and the concentrations of standard polysaccharides derived by PMP. Briefly, PMP-marked TPS and LBPS stock solutions with concentration gradients of 1.0, 0.5, 0.4, 0.3, 0.2, 0.1, 0.05 and 0.01 mg/mL, and 0.3, 0.2, 0.1, 0.05, 0.01 and 0.005 mg/mL were prepared and their chromatographic

retentions were surveyed with the aforementioned conditions. Each sample was tested in triplicate and the weighted peak area was used for plotting standard curves, then the concentrations of polysaccharides in extracts were deduced by linear regression equations.

Reusability tests of MNPs@B(OH)₂

The recyclability of MNPs@B(OH)₂ was investigated by consecutive extraction and desorption 10 times. In detail, 80.0 mg MNPs@B(OH)₂ was dispersed into 20 mL PB containing 3.0 mg/mL TPS, then incubation for 1 h at room temperature. After that, the materials were magnetically collected and washed with 5 mL PB for 5 min, followed by desorption for 0.5 h with 1 mL HAc aqueous solution (0.1 M). Finally, the supernatants were separately collected after magnetic isolation. After color development by phenyl-sulfuric acid method, their UV-vis spectra were tested and digital photos were recorded. Such an extraction-elution process was repeated for 10 cycles. A pre-equilibrium period of 1 h by PB (10 mL) was adopted for MNPs@B(OH)₂ between two extractions.

Antioxidant capacity assessed by DPPH radical scavenging assay

Two aliquots of 1.0 mL ethanol solution containing 0.06 mg/mL DPPH were, respectively, mixed with 0.3 mL TPS and LBPS solution (dissolved in ethanol, and both with a concentration of 0.5 mg/mL). The DPPH solution combined with an equal volume of ethanol was used as the control group. After incubation in the dark for appropriate periods (0, 1, 3, 5, 10, 20, 30, 45 and 60 min), the digital photos were recorded using a smartphone and the UV-vis spectra were measured on a spectrophotometer. The radical scavenging activities of TPS and LBPS were evaluated by the following expression:

$$\text{Radical scavenging activity (\%)} = \left(1 - \frac{A_T}{A_C}\right) \times 100$$

In which, A_T and A_C were, respectively, on behalf of the absorbance of polysaccharides-treated group and control group (without additives).

Cell culture and antitumor activity evaluation

MCF-7 cell was cultured in RPMI-1640 medium supplemented with 10% fetal bovine serum at 37 °C in a humidified chamber containing 5% CO₂. A549 and DU145 cells were cultured in DMEM medium with 10% fetal bovine serum at 37 °C in a humidified chamber containing 5% CO₂. All the cell experiments were implemented when the confluence reached ~80%. MTT assays and trypan blue staining experiments were adopted to estimate cell viability and apoptosis, respectively.

Details for MTT assay: The cells cultured in 96-well microplate were washed with 1 × PBS three times, followed by supplementing with relevant culture medium containing polysaccharide extracts with different concentrations ranging from 0 (control), 0.25, 1.0, 1.5, 2.5 to 5.0 mg/mL (200 µL per well). After culturing for another 24 h, the culture medium was removed and the remaining cells in microplate were cultured with PBS containing 5.0 mg/mL 3-(4,5-dimethylthiazol-2-yl)-2,5-diphenyltetrazolium bromide (MTT, 50 µL per well), and then cultured for 4 h. The remaining MTT reagent was discarded and 100 µL DMSO was supplemented into each well, and then slowly shaken for 10 min to dissolve the formazan in cells. Finally, the absorbance of the DMSO solutions was determined at 492 nm on a Synergy H1M microplate reader (BioTek,

Extraction and bioactivities of polysaccharides

Winooski, VT, USA). The formula given below was utilized to calculate the cell viability (%):

$$\text{Cell viability} = \frac{A_T - A_b}{A_C - A_b} \times 100\%$$

Herein, A_T , A_C and A_b represented the absorbance value of treatment group, control group (cells without additives) and 96-well microplate substrate, respectively.

Trypan blue staining trials were performed as follows: The preculture with polysaccharide extract-added medium was the same as above, but only the cells cultured by the medium containing 0 and 5.0 mg/mL polysaccharide extractions were selected for staining and comparison. The pretreated cells were subsequently stained by 0.4% (wt%) trypan blue solution for 3 min, then microscopic images of the resulting cells were recorded on an inverted fluorescence microscope (Sunny Optical XD-FRL, 10 × objectives).

Results and discussion

Preparation and characterization of MNPs@B(OH)₂

Two steps were concluded for the preparation of MNPs@B(OH)₂, namely the synthesis of amino group-capped MNPs (bare MNPs) and boronic acid functionalization of bare MNPs. The synthetic route was illustrated in Supplemental Fig. S1, in which bare MNPs were fabricated *via* the one-step solvothermal method^[4,5], and then the boronic acid modification was carried out in terms of Schiff-base reaction between amino groups onto bare MNPs and the formyl groups of FPBA^[16,17]. Transmission electron microscopy (TEM) characterization indicated that both bare MNPs and MNPs@B(OH)₂ were of fine water dispersibility and regular morphology, and the particle size of bare MNPs and MNPs@B(OH)₂ was respectively estimated to be ca. 70~120 nm and 80~140 nm from TEM and DLS analysis (Fig. 2a – c). Magnetic separation of MNPs@B(OH)₂ could be easily achieved by external magnetic field (inset in

Fig. 2b), which facilitated the operations of SPE. The slight increase in particle size of MNPs@B(OH)₂ as compared with bare MNPs might be caused by the repeated magnetic separation during the post modification of boronic acid (FPBA).

The boronic acid functionalization was firstly evaluated by UV-vis spectrometry, and the characteristic absorption at 260 nm (produced by aromatic ring) of MNPs@B(OH)₂ suggested that FPBA was successfully modified onto MNPs (Fig. 2d). FT-IR was further applied to confirm this claim. As seen in Fig. 2e, wide absorption band at ~3,413 cm⁻¹ should be allotted to the stretching vibration of -OH or -NH₂; the bands at 2,921 and 2,849 cm⁻¹ should be assigned to the stretching vibration of C-H in methylene groups; the peak at 1,568 cm⁻¹ should be attributed to the in-plane bending vibration of N-H of secondary amine while the peaks at 1,347 cm⁻¹ was associated with the C-B vibrations; 1,158 and 1,073 cm⁻¹ indicated the existence of C-N; the bands at 947 and 856 cm⁻¹ could be, respectively, identified by the out-of-plane deformation vibration of hydroxyl group in boronic acid group and the *p*-disubstitution of the aromatic ring. These results were in agreement with previous literature reports^[5,18] and affirmed that the post-modification of FPBA was workable. Additionally, the greater mass loss of MNPs@B(OH)₂ than that of bare MNPs (4.5% vs 1.1%) in TGA tests (Fig. 2f) also validated the reasonability of this claim.

Boronate affinity-mediated MSPE

Boronate affinity has been well proved to be of excellent class recognition selectivity toward *cis*-diol containing compounds over non-*cis*-diol compounds^[10,19–21]. Thus, the binding selectivity of MNPs@B(OH)₂ was firstly examined using cytidine, guanosine, adenosine, deoxyguanosine and deoxyadenosine as model analytes, among which cytidine, guanosine and adenosine were *cis*-diol compounds. As exhibited in Fig. 3a & b, only limited extraction capacity of bare MNPs could be observed toward model analytes, as contrasts, MNPs@B(OH)₂

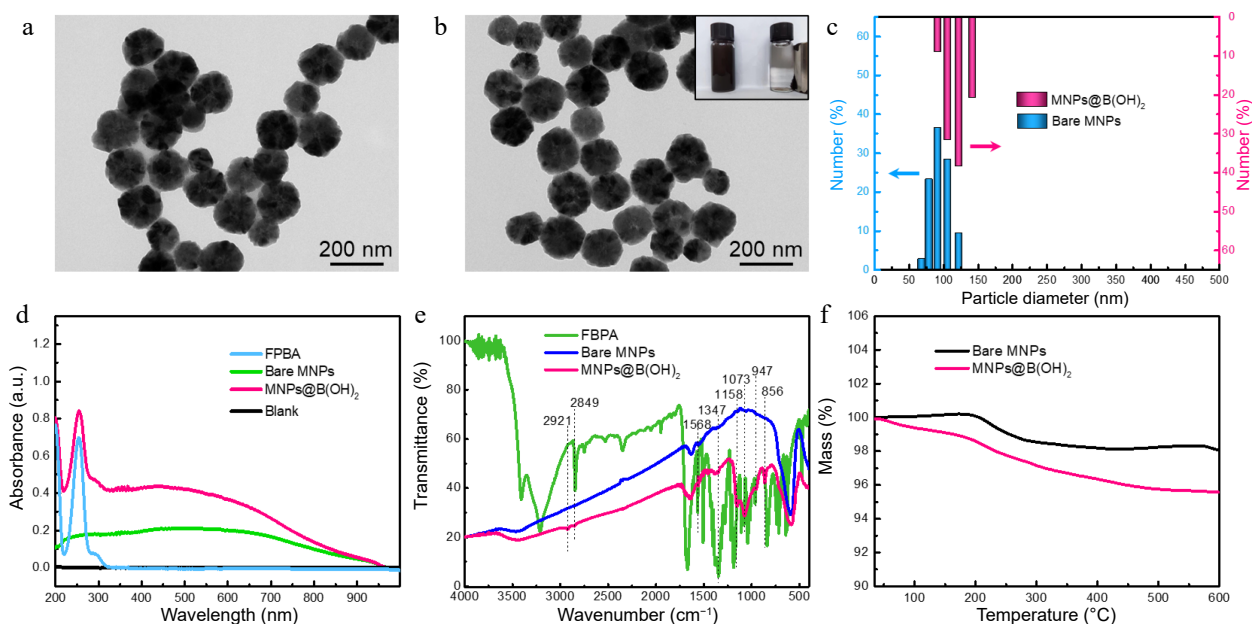


Fig. 2 TEM characterization of (a) bare MNPs and (b) boronic acid-grafted MNPs, along with their particle size distributions analyzed by (c) DLS; (d) UV-vis spectra, (e) FT-IR spectra, and (f) TGA tests of MNPs materials with or without modification by FPBA. Inset in (b) was the digital photo showing the magnetic separation behavior of MNPs@B(OH)₂ by an external magnet.

displayed high binding ability toward cytidine, guanosine and adenosine, giving an equilibrium binding capacity (Q_e) of 81.44 vs 1.87 μg , 230.41 vs $-3.21 \mu\text{g}$, and 240.92 vs 57.35 μg , respectively, which suggested that MNPs@B(OH)_2 were of good recognition selectivity toward *cis*-diol compounds against non-*cis*-diol compounds. The influence of pH on the binding capacity of MNPs@B(OH)_2 was given in Fig. 3c & d, and the results indicated that optimal binding performance could be achieved at pH 7.5~8.5, which could be rationalized by the fact that boronate affinity effect would be active at such a pH around pK_a of FPBA^[22,23]. Such a weak alkaline working pH is beneficial to maintain the structural stability of polysaccharide. Binding dynamics assay declared that the binding equilibrium could be reached within 10 min (Fig. 3e & f), which is consistent with the rapid binding feature of boronate affinity^[10], and also provided a reference for selection of extraction time during polysaccharide MSPE. These findings revealed that the binding between MNPs@B(OH)_2 and *cis*-diol compounds was dominated by

boronate affinity effect, laying the foundation for upcoming BA-MSPE of polysaccharides.

The extraction performance of bare MNPs and MNPs@B(OH)_2 was compared using SPS, PPS, LBPS and TPS as model polysaccharides, and the results were provided in Fig. 4a & b. Obviously, the equilibrium binding capacity (Q_e) of MNPs@B(OH)_2 was higher than that of bare MNPs in all cases, and a deeper color also appeared after color development by the phenol-sulfuric acid method, which demonstrated that boronate affinity was activated and essential for MSPE of polysaccharides. Zeta (ζ) potential tests disclosed that MNPs@B(OH)_2 were negatively charged at the given conditions (phosphate buffer solution with pH 8.5) while the ζ potentials of PPS-/TPS-extracted MNPs@B(OH)_2 were slightly enhanced (Supplemental Fig. S2), offering a value of $-41.6 \pm 2.68 \text{ mV}$, $-38.3 \pm 3.12 \text{ mV}$, and $-38.7 \pm 2.26 \text{ mV}$, respectively. The negative charge of MNPs@B(OH)_2 ought to ascribe to the formation of boronic anions with the boron in its tetragonal hybridization^[24] at pH 8.5 while the

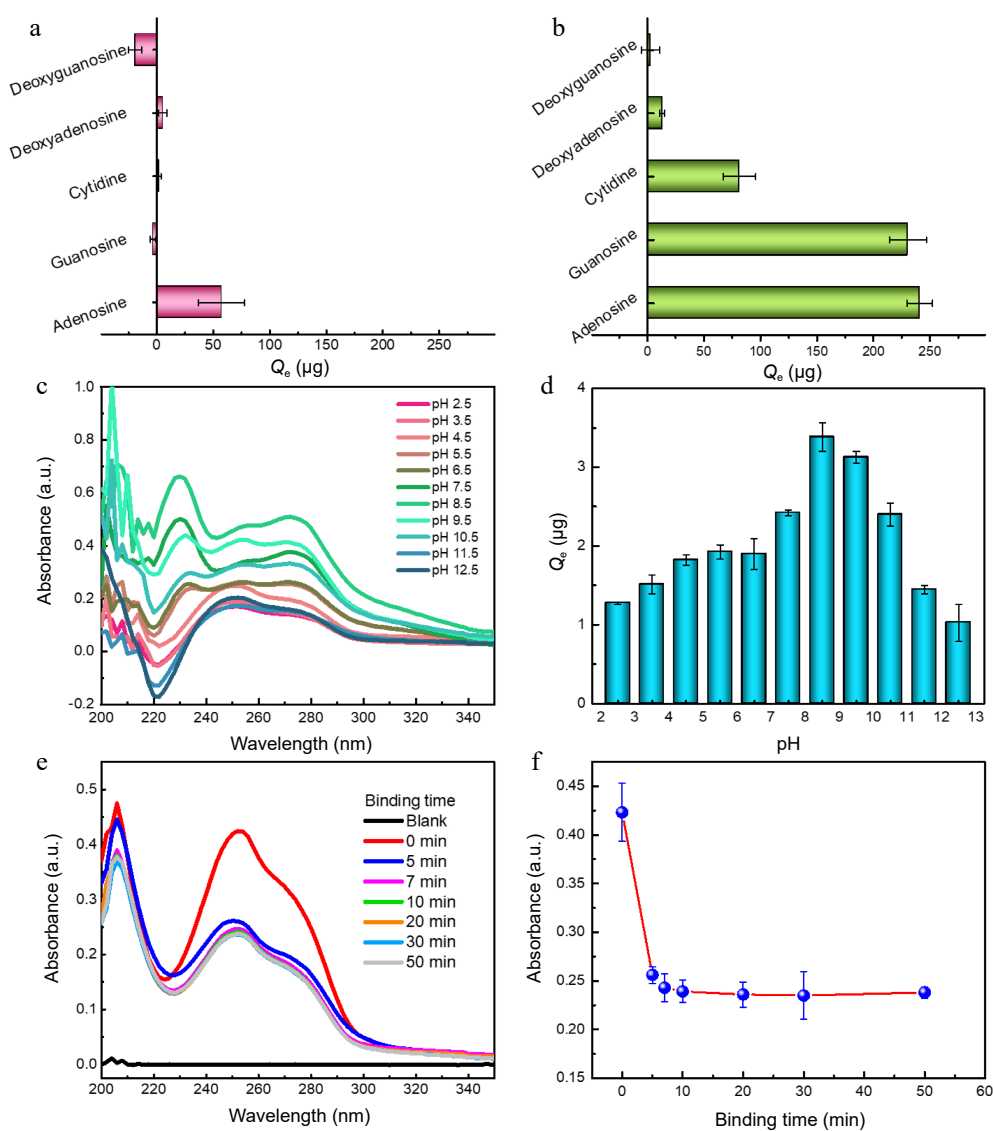


Fig. 3 Binding selectivity of (a) bare MNPs and (b) MNPs@B(OH)_2 toward five model compounds; Typical UV-vis spectra of guanosine extracted by MNPs@B(OH)_2 at (c) different pH and their (d) quantitative comparison; (e) UV-vis spectra of guanosine in supernatants after extraction by MNPs@B(OH)_2 at different extraction time, and (f) the absorbance of guanosine in supernatants as a function of extraction time. All tests were carried out at least three times in parallel.

Extraction and bioactivities of polysaccharides

increased surface potential after extraction of polysaccharides could be clarified by the electroneutrality and relatively large molecular weight of polysaccharides, which affect the surface charge of MNPs@B(OH)_2 . These results proved that MNPs@B(OH)_2 -mediated MSPE of polysaccharides was workable, and boronic acid played a vital role in this process.

Adsorption isotherm was further used to assess the binding properties of MNPs@B(OH)_2 using tea polysaccharide (TPS) as a model analyte, in which the standard curve method presented in Supplemental Fig. S3 and Supplemental Table S1 was utilized for quantification, and the Hill equation^[25–27] was selected to nonlinearly fit the data. The theoretical maximum binding capacity (Q_{max}) of MNPs@B(OH)_2 toward TPS was deduced to be 12.93 $\mu\text{g}/\text{mg}$ (Fig. 4c), accompanying a dissociation constant (K_d) of 4.72 mg/mL or $4.63 \times 10^{-3} \sim 4.63 \times 10^{-6}$ M ($R^2 = 0.9896$, the molecular weight of TPS from tea leaves was ca. 1.02~1020 kDa according to literature reports^[28]). Such a K_d level was lower than that of boronic acid and small molecular *cis*-diol compounds (K_d was usually on the order of magnitudes of $10^{-1} \sim 10^{-4}$ M^[22–24]), indicating higher binding force between boronic acid and polysaccharides as compared with the binding between boronic acid and small molecular *cis*-diol compounds. This outcome would be explained by the plenty of 1,2- and 1,3-*cis*-diol structures of polysaccharide and consequently formed positive synergetic effects by the multi-sites

binding between boronic acid and polysaccharide. It also implied the correctness of the possible binding mechanism proposed in Fig. 1. Moreover, a fine linear correlation ($y = 0.0445x - 0.0029$, $R^2 = 0.9579$) between the Q_e of MNPs@B(OH)_2 and TPS concentrations could be found in the concentration range of 0.05~6.0 mg/mL, and a good color evolution of polysaccharide extractives after color development by phenol-sulfuric acid method also emerged as polysaccharide concentrations increased, paving the way for quantification of BA-MPSE and giving a guideline for the consumption of materials in real applications.

Extraction of polysaccharides from real-world beverage plants

The above-mentioned results encouraged us to explore the feasibility of polysaccharides BA-MSPE in real beverage plants. *Lycium barbarum*, tea leaves (green tea) and soybeans were devoted as real plant samples, and the extraction of polysaccharides from these plants by bare MNPs and MNPs@B(OH)_2 was compared in Fig. 5. After chromogenesis by phenol-sulfuric acid method, strong absorption of leaching liquors at 488 nm demonstrated that polysaccharides were successfully released from plant samples. Higher absorbance of extractives by MNPs@B(OH)_2 than those by bare MNPs declared better MSPE performance of MNPs@B(OH)_2 (Fig. 5a~c), giving the binding capacity 4.6 times as high in MNPs@B(OH)_2 as in bare

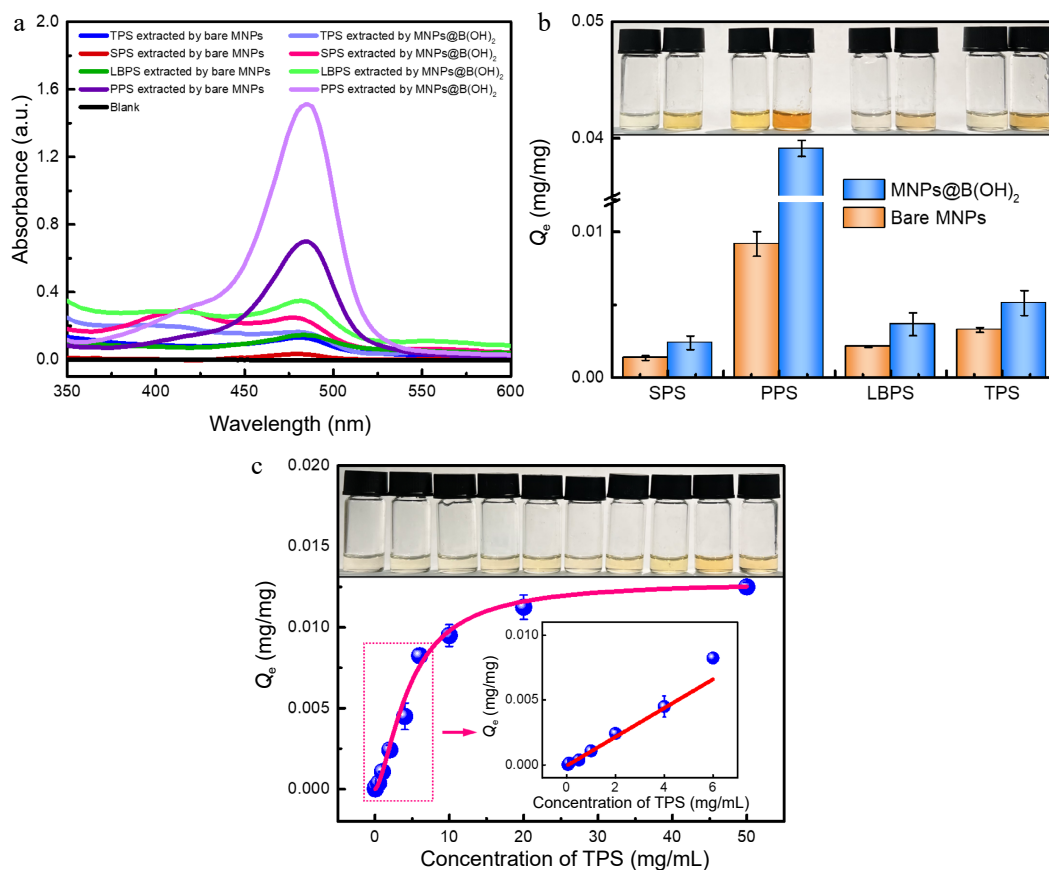


Fig. 4 UV-vis spectra of four polysaccharide extractives by different MNPs after (a) color development by the phenol-sulfuric acid method, and the (b) equilibrium binding capacity of bare MNPs and MNPs@B(OH)_2 toward four model polysaccharides, all with a concentration of 1.0 mg/mL; (c) Adsorption isotherms for TPS binding to MNPs@B(OH)_2 . Insets in (b) and (c): digital photos of polysaccharide extractives (derived by phenol-sulfuric acid chromogenic reaction) with the same order as relevant horizontal axis. Diagrams inserted in (c): linear fitting in the working range of 0.05~6.0 mg/mL ($y = 0.0445x - 0.0029$, $R^2 = 0.9579$). All measurements were repeated in triplicate at least for quantitative calculations.

MNPs (LBPS, Fig. 5d). The possible reason for the variation in the relative binding capacity of MNPs and MNPs@B(OH)₂ in Figs 4b & 5d would be attributed to the fact that the initial concentrations of standard polysaccharides and the polysaccharides in leaching liquors of real beverage plants were different. The digital photos of freeze-dried polysaccharide extractives and standard polysaccharide samples were showed in Supplemental Fig. S4, and the similar appearance and colors between them also implied that it was practicable to extract polysaccharides in real beverage plants by MNPs@B(OH)₂.

The relative purities of TPB and LBPS extractives were roughly estimated by UV-vis spectrometry using standard polysaccharides as benchmarks and standard curve method for quantification. As displayed in Fig. 5e, the same characteristic bands at ~488 nm and the similar colors between polysaccharide extractives and standard polysaccharide samples after color development by phenol-sulfuric acid chromogenic reaction demonstrated that polysaccharides were efficiently extracted by MNPs@B(OH)₂, showing a deduced relative purity of (56.8 ± 0.9)% and (69.1 ± 1.9)% for LBPS and TPS (Supplemental Table S1), respectively. HPLC, a powerful tool for quantification of polysaccharides^[29,30], was applied to further confirm these outcomes using PMP labeling reaction for the pre-column derivatization of polysaccharides. Standard curve method showed in Supplemental Fig. S5 and Supplemental Table S2 were employed to infer the content of polysaccharides in extracts. As shown in Fig. 5f, the similar chromatographic retention behaviors could be found between polysaccharide extractives and standard polysaccharides, and the

peaks at retention time near 28 min (light violet area in Fig. 5f) could be allotted to the chromatographic curves of polysaccharides by virtue of the mapping between peak area and concentrations, which further verified that polysaccharides were effectively extracted by MNPs@B(OH)₂. The relative purities were, respectively, (43.1 ± 1.3)% and (59.2 ± 5.3)% for LBPS and TPS. Higher purities produced by UV-vis spectrometry than those from HPLC might be attributed to the existence of unknown impurities, while such a positive error could be avoided thanks to the separation effect of HPLC. Although the purity level was not so high, it was acceptable considering that only once extraction was implemented in such a facile way of BA-MSPE.

FT-IR spectrometry was used for the structure identification of extracted polysaccharides. As seen in Supplemental Fig. S6, the absorption bands at 3429/3413 cm⁻¹ and 2931/2923 cm⁻¹ were assigned to the stretching vibration of -OH groups and C-H (in -CH₂- groups); the band at 1650 cm⁻¹ was due to the stretching vibration of aldehydic carbonyl; the band at 1405/1409 cm⁻¹ was on count of the deformation vibration of -CH₂- groups; the peaks at 1248/1251 cm⁻¹ and 1023/1054 cm⁻¹ were attributed to the stretching vibration of C-OH side groups or C-O-C glycosidic bond vibrations, suggesting the possible structure of pyranose ring in sugar residues; the absorption bands at 937/944 cm⁻¹ and 849/850 cm⁻¹ were, respectively, caused by β- and α-glycosidic bonds. These results are in agreement with the literature reports^[15,31], and also double-checked the validity of BA-MSPE for polysaccharides. The main absorption bands were basically the same for TPS and LBPS, indicating their primary chemical structures were similar. Meanwhile,

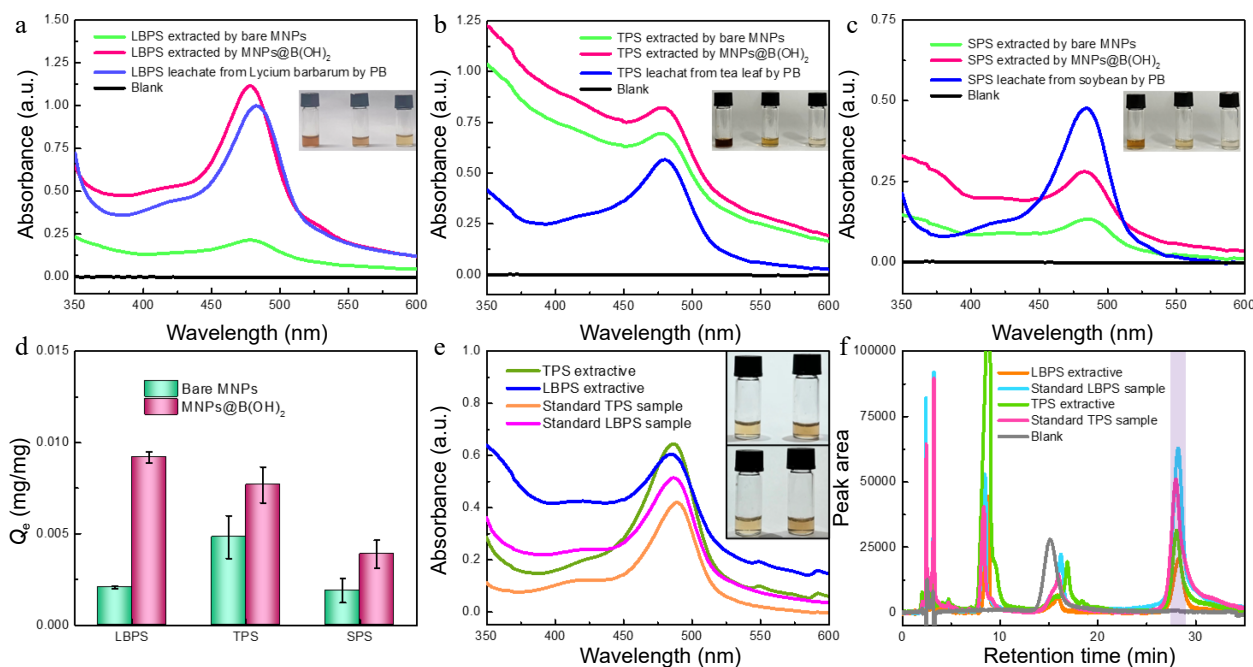


Fig. 5 UV-vis spectra of polysaccharide leaching liquors and extracts from (a) *Lycium barbarum*, (b) tea leaves and (c) soybeans by different materials. The comparison in extraction performance of bare MNPs and MNP@B(OH)₂ (d, $n = 3$); (e) UV-vis spectra of TPS and LBPS extractives (1.0 mg/mL) and standard polysaccharide solutions (0.5 mg/mL); (f) HPLC chromatograms of TPS and LBPS extractives (1.0 mg/mL for TPS, and 0.5 mg/mL for LBPS) and standard polysaccharide solutions (0.5 mg/mL for TPS, and 0.3 mg/mL for LBPS) after labelling with PMP, in which light violet zone indicated the peak position of polysaccharides. Insets in (a)–(c) were, respectively, the digital photos of relevant polysaccharides obtained in different pathways after color development with phenol-sulfuric acid chromogenic method, and the order was leachates and the extractives by MNPs@B(OH)₂ and bare MNPs from left to right. The inset in (e) was the photos of polysaccharide extractives (top) and standard polysaccharide samples (bottom) of TPS (left) and LBPS (right) with the same concentrations as UV-vis spectra tests. All UV-vis spectrograms were obtained after phenol-sulfuric acid chromogenic reaction.

Extraction and bioactivities of polysaccharides

the similarity in characteristic peaks between polysaccharide extracts and standard polysaccharide samples suggested that the structural integrities of extracted polysaccharides were well maintained, which would benefit from the mild extraction conditions during the process of BA-MSPE.

HPLC analysis was applied to roughly estimate the monosaccharide composites of extracted LBPS and TPS. The polysaccharides were first hydrolyzed by the trifluoroacetic acid method and subsequently labeled by PMP prior to sample loading. As presented in Supplemental Fig. S7, six chromatographic peaks could be found from the chromatographic curves of TPS and LBPS, and the principal compositions of xylose (Xyl), arabinose (Ara), glucose (Glc), and galactose (Gal) could be identified. Detailly, peaks 1~6 would be respectively assigned to Xyl, Ara, Xyl, Ara, Glc and Gal for LBPS, and Xyl, Xyl, Ara, Glc, Ara and Gal for TPS as compared with the retention of monosaccharides, giving peak area percentages of 1.5%, 1.5%, 14.8%, 14.2%, 22.1% and 45.9% for LBPS, and 14.4%, 42.4%, 20.1%, 6.3%, 5.0% and 11.8% for TPS. Since no UV absorption signal could be produced by monosaccharides themselves, it was rational to roughly estimate the relative content of monosaccharides by peak area percentages. It was clear that the predominant monosaccharides were Glc and Gal in LBPS, and Xyl and Ara in TPS, which is basically consistent with the results reported in the literature^[28,32,33]. The content of Xyl in TPS was somewhat different from that reported in the literature^[28], and the reason might be related to the difference of tea categories, origin, as well as the hydrolysis conditions.

The relationship between extraction capacity and the dosage of MNPs@B(OH)₂ used for MSPE was furtherly probed using TPS and LBPS as model polysaccharides, and the consequences were presented in Supplemental Fig. S8. Although the relative binding capacity of MNPs@B(OH)₂ was not so high (Fig. 5d) due to their large specific gravity (chemical compositions of MNPs were mainly Fe₃O₄ and/or Fe₂O₃^[34]), the extracted amounts of two polysaccharides were linearly enhanced as the consumption of MNPs@B(OH)₂ increased from 10 to 150 mg (Supplemental Fig. S8a–c), giving a linear regression equation of $y = 0.0056x + 0.4535$ ($R^2 = 0.9392$) for TPS, and $y = 0.0073x + 0.2953$ ($R^2 = 0.9294$) for LBPS, respectively. Correspondingly, the colors of polysaccharide extractives were gradually deepened as the increase of MNPs@B(OH)₂ loading amounts (Supplemental Fig. S8d). Clearly, to some extent, such a dosage-dependent extraction capacity remedied the foible of relatively low binding capacity of MNPs@B(OH)₂, and provided a guidance for their dosage selection in real applications.

The reusability of MNPs@B(OH)₂ for BA-MSPE was further explored using TPS as a model polysaccharide, and the results are showed in Supplemental Fig. S9. The fluctuation in binding capacity of MNPs@B(OH)₂ after continuous extraction and desorption ten times was less than 13%, demonstrating an acceptable recyclability of MNPs@B(OH)₂ for polysaccharide extraction. Likewise, after color development with phenyl-sulfuric acid method, the colors of TPS extractives obtained by ten consecutive extractions were very close, which confirms the above-stated claim.

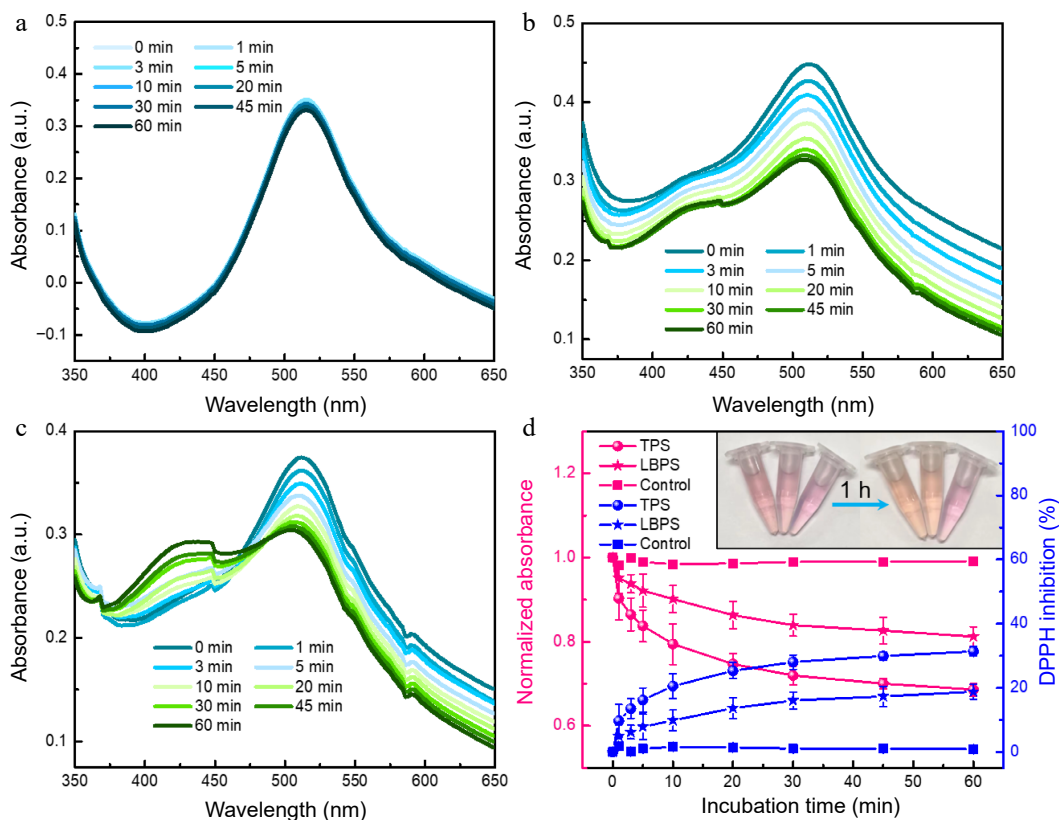


Fig. 6 UV-vis spectra of (a) DPPH, (b) TPS- and (c) LBPS- added DPPH obtained at incubation time ranging from 0 to 60 min. Antioxidant ability of TPS and LBPS assessed by DPPH scavenging activity assay (d, $n = 3$). The final concentration of both TPS and LBPS added in DPPH was 0.2 mg/mL.

Antioxidant and antitumor bioactivities of extracted polysaccharides

Antioxidant activity of the obtained TPS and LBPS extracts by MNPs@B(OH)₂ was investigated by DPPH radical scavenging assays^[35–37]. As shown in Fig. 6, no obvious change could be observed in the absorbance of DPPH after monitoring continuously for 1 h in the absence of polysaccharide ($\Delta A < 1.9\%$, Fig. 6a & d), by contrast, the absorbance of DPPH was significantly decreased in the presence of TPS and LBPS even their concentration as low as 0.2 mg/mL (Fig. 6b–d), showing a free radical scavenging rate of 31.4% and 18.8%, respectively.

Correspondingly, the color of DPPH solution without the addition of polysaccharides was stable while the color variations of polysaccharide-added DPPH were eye-catching enough. These findings certified that the polysaccharides extracted by MNPs@B(OH)₂ were of fine antioxidant activity. The possible reasons for stronger antioxidant capability of TPS than that of LBPS could ascribe to its higher relative purity, broader distribution in molecular weight^[28] and abundant active functional groups^[38].

The antitumor activities of LBPS and TPS were subsequently probed by microscopic imaging, MTT trials, along with trypan

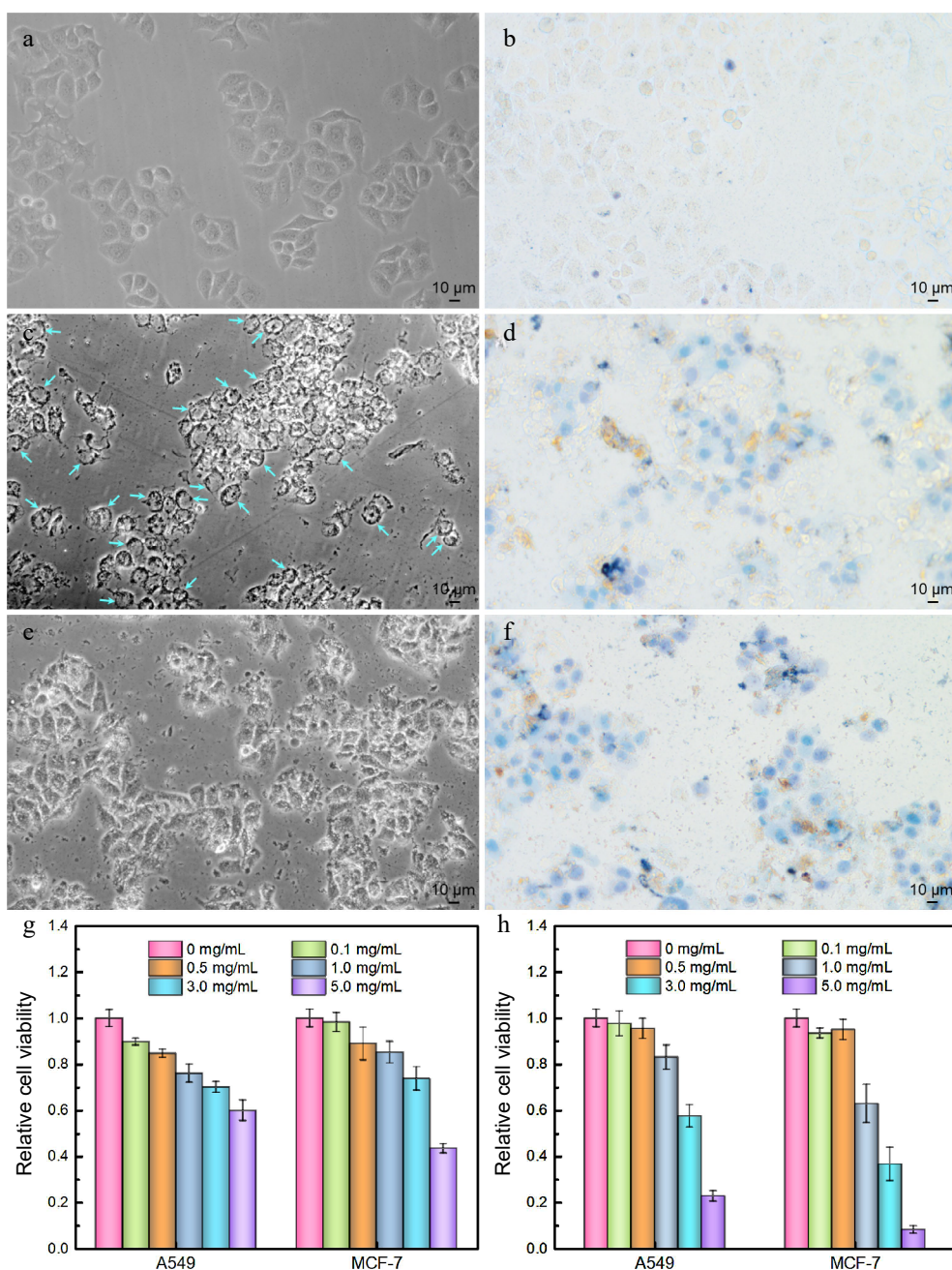


Fig. 7 Antitumor activities of polysaccharide extracts assessed by optical microscopic imaging (a) – (f) using MCF-7 cells as a model cell line and (g), (h) MTT assays. (a) Cell imaging of control group, (b) trypan blue stained control group, (c) LBPS-treated group, (d) trypan blue stained LBPS-treated group, (e) TPS-treated group, and (f) trypan blue stained TPS-treated group. The dosage of TPS and LBPS in (c) – (f) was set as 5.0 mg/mL. Relative cell viabilities of A549 and MCF-7 cells after administrating by (g) LBPS and (h) TPS by MTT assays. Blue arrows in (c) on behalf of the typical vacuolated cells.

Extraction and bioactivities of polysaccharides

blue staining assays^[39] using A549 and MCF-7 as representative carcinoma cell lines, and the results were presented in [Supplemental Figs 7 & S10](#). Microscopic imaging implied that the cells morphology changed significantly, focusing on cell shrinkage, deteriorated adhesion ability, and the abnormal distribution of intracellular contents. Irreversible vacuolation emerged widely in both A549 and MCF-7 cells under the culture condition in the presence of LBPS ([Fig. 7c, d, Supplemental Fig. S10c, d](#)), while cell disruption was more distinct after culturing with TPS ([Fig. 7e, f, Supplemental Fig. S10e, f](#)), and a large number of cell fragments could be found in this case, suggesting cells were dying and cell functional statuses changed. These phenomena might be closely related with different apoptosis pathways induced by TPS and LBPS. TPS have been proved to be of lysosomes targetability and induced apoptosis by a lysosomal-mitochondrial pathway mediated caspase cascade^[40], while the inhibitions in proliferation, migration and survival of tumor cells by LBPS were testified to be related with Pi3K/AKT signaling pathway^[41]. Furthermore, all cells were well stained by trypan blue after administrating by LBPS and TPS ([Figs 7d, f, Supplemental Fig. S10d, f](#)), as controls, only a few cells were stained in control groups, which further confirmed that polysaccharide extracts were of antitumor activity and caused cell death. The relative cell viabilities were profiled by MTT assays and the results were given in [Fig. 7g, h](#). An obvious dosage-dependent cytotoxicity could be observed for both LBPS and TPS extractives, showing a relative cell survival rate less than 60.0% and 22.8% for A549 cells, and 43.4% and 8.2% for MCF-7 cells after respectively treating by LBPS and TPS with an equal concentration of 5.0 mg/mL. The higher cell mortality rate induced by TPS as compared with LBPS might be thanks to its relatively higher purity obtained during BA-MSPE. These findings were consistent with the results of literature reports^[40–43], and confirmed the reliability of antitumor activities of polysaccharide extractives.

Conclusions

Boronic acid-functionalized magnetic nanoparticles (MNPs@B(OH)₂) have been prepared and used as sorbents for boronate affinity-mediated MSPE of polysaccharides in this work. Boronate affinity effect and its work parameters were investigated, the mechanism for the binding of polysaccharides by MNPs@B(OH)₂ was discussed, and the extraction conditions were also optimized. Three polysaccharides, including TPS, LBPS and SPS, were successfully extracted from relevant real-world beverage plants, and the main active ingredients in extracts were identified by several instrumental analysis techniques, such as UV-vis/FT-IR spectrometry and HPLC. In the end, the extracted TPS and LBPS were experimentally proven to be of fine antioxidant and antitumor bioactivities in terms of DPPH radical scavenging experiments, trypan blue staining, as well as MTT assays. Since the operations of BA-MSPE were straightforward and do not necessitate the use of organic solvents or other intricate impurities elimination steps during BA-MSPE, coupled with the fine recyclability of MNPs@B(OH)₂, this approach may have more potential for the simple separation and purification of *cis*-diol containing compounds in the fields of food and agricultural product processing.

Acknowledgments

This work was funded by the National Natural Science Foundation of China (Grant No. 21904003), the University Scientific Research Project of Anhui Province (2022AH050296), the Natural Science Foundation of Anhui Province (Grant No. 2108085QB85), the Open Project of Anhui Engineering Technology Research Center of Biochemical Pharmaceutical (Bengbu Medical College) (Grant No. 2022SYKFZ02), and the Student Research Training Program of Anhui University of Technology (Grant No. 202210360031, 202210360038).

Conflict of interest

The authors declare that they have no conflict of interest.

Supplementary Information accompanies this paper at (<https://www.maxapress.com/article/doi/10.48130/BPR-2023-0014>)

Dates

Received 19 April 2023; Revised 7 May 2023; Accepted 11 May 2023; Published online 14 June 2023

References

- Xie L, Shen M, Wang Z, Xie J. 2021. Structure, function and food applications of carboxymethylated polysaccharides: a comprehensive review. *Trends in Food Science & Technology* 118:539–57
- Masci A, Carradori S, Casadei M A, Paolicelli P, Petralito S, et al. 2018. *Lycium barbarum* polysaccharides: Extraction, purification, structural characterisation and evidence about hypoglycaemic and hypolipidaemic effects. A review. *Food Chemistry* 254:377–89
- Huang Y, Chen H, Zhang K, Lu Y, Wu Q, et al. 2022. Extraction, purification, structural characterization, and gut microbiota relationship of polysaccharides: a review. *International Journal of Biological Macromolecules* 213:967–86
- Wang S, Li W, Sun P, Xu Z, Ding Y, et al. 2020. Selective extraction of myoglobin from human serum with antibody-biomimetic magnetic nanoparticles. *Talanta* 219:121327
- Bie Z, Chen Y, Ye J, Wang S, Liu Z. 2015. Boronate-affinity glycan-oriented surface imprinting: a new strategy to mimic lectins for the recognition of an intact glycoprotein and its characteristic fragments. *Angewandte Chemie International Edition* 54:10211–15
- Wang X, Li G, Row KH. 2017. Magnetic graphene oxide modified by imidazole-based ionic liquids for the magnetic-based solid-phase extraction of polysaccharides from brown alga. *Journal of Separation Science* 40:3301–10
- Liu Z, He H. 2017. Synthesis and applications of boronate affinity materials: from class selectivity to biomimetic specificity. *Accounts of Chemical Research* 50:2185–93
- Li D, Chen Y, Liu Z. 2015. Boronate affinity materials for separation and molecular recognition: structure, properties and applications. *Chemical Society Reviews* 44:8097–123
- Chen Y, Huang A, Zhang Y, Bie Z. 2019. Recent advances of boronate affinity materials in sample preparation. *Analytica Chimica Acta* 1076:1–17
- Wang S, Ye J, Bie Z, Liu Z. 2014. Affinity-tunable specific recognition of glycoproteins via boronate affinity-based controllable oriented surface imprinting. *Chemical Science* 5:1135–40
- Wang S, Ye J, Li X, Liu Z. 2016. Boronate affinity fluorescent nanoparticles for Förster resonance energy transfer inhibition assay of *cis*-diol biomolecules. *Analytical Chemistry* 88:5088–96
- Fan Y, Zhou X, Huang G. 2022. Preparation, structure, and properties of tea polysaccharide. *Chemical Biology & Drug Design* 99:75–82

13. Pan X, Chen Y, Zhao P, Li D, Liu Z. 2015. Highly efficient solid-phase labeling of saccharides within boronic acid functionalized mesoporous silica nanoparticles. *Angewandte Chemie International Edition* 54:6173–76
14. Wang W, Chen F, Wang Y, Wang L, Fu H, et al. 2018. Optimization of reactions between reducing sugars and 1-phenyl-3-methyl-5-pyrazolone (PMP) by response surface methodology. *Food Chemistry* 254:158–64
15. Yang X, Wei S, Lu X, Qiao X, Simal-Gandara J, et al. 2021. A neutral polysaccharide with a triple helix structure from ginger: characterization and immunomodulatory activity. *Food Chemistry* 350:129261
16. Wang S, He Z, Li W, Zhao J, Chen T, et al. 2020. Reshaping of pipette tip: a facile and practical strategy for sorbent packing-free solid phase extraction. *Analytica Chimica Acta* 1100:47–56
17. Wang S, Li W, Yuan Z, Jin Q, Ding Z, et al. 2022. Semiquantitative naked-eye detection of synthetic food colorants using highly-branched pipette tip as an all-in-one device. *Analytica Chimica Acta* 1211:339901
18. Wang H, Bie Z, Lü C, Liu Z. 2013. Magnetic nanoparticles with dendrimer-assisted boronate avidity for the selective enrichment of trace glycoproteins. *Chemical Science* 4:4298–303
19. Wang S, Wen Y, Wang Y, Ma Y, Liu Z. 2017. Pattern recognition of cells via multiplexed imaging with monosaccharide-imprinted quantum dots. *Analytical Chemistry* 89:5646–52
20. Ye J, Chen Y, Liu Z. 2014. A boronate affinity sandwich assay: an appealing alternative to immunoassays for the determination of glycoproteins. *Angewandte Chemie International Edition* 53:10386–89
21. Bi X, Liu Z. 2014. Enzyme activity assay of glycoprotein enzymes based on a boronate affinity molecularly imprinted 96-well microplate. *Analytical Chemistry* 86:12382–89
22. Lü C, Li H, Wang H, Liu Z. 2013. Probing the interactions between boronic acids and *cis*-diol-containing biomolecules by affinity capillary electrophoresis. *Analytical Chemistry* 85:2361–69
23. Otsuka H, Uchimura E, Koshino H, Okano T, Kataoka K. 2003. Anomalous binding profile of phenylboronic acid with N-acetylneuraminic acid (Neu5Ac) in aqueous solution with varying pH. *Journal of the American Chemical Society* 125:3493–502
24. Djanashvili K, Frullano L, Peters JA. 2005. Molecular recognition of sialic acid end groups by phenylboronates. *Chemistry – A European Journal* 11:4010–18
25. Wang S, Wang H, Yuan Z, Li M, Gao H, et al. 2022. Colorimetry combined with inner filter effect-based fluorometry: a versatile and robust strategy for multimode visualization of food dyes. *ACS Applied Materials & Interfaces* 14:57251–64
26. Wang S, Zhang L, Jin Q, Xu Z, Zhao J, et al. 2022. Filter paper-based colorimetric analysis: an instrument-free strategy for semiquantitative naked-eye detection of food colorants. *Food Chemistry* 390:133087
27. Wang S, Wang H, Ding Y, Li W, Gao H, et al. 2022. Filter paper- and smartphone-based point-of-care tests for rapid and reliable detection of artificial food colorants. *Microchemical Journal* 183:108088
28. Chen G, Yuan Q, Saeeduddin M, Ou S, Zeng X, et al. 2016. Recent advances in tea polysaccharides: extraction, purification, physico-chemical characterization and bioactivities. *Carbohydrate Polymers* 153:663–78
29. Sknepnek A, Tomić S, Miletić D, Lević S, Čolić M, et al. 2021. Fermentation characteristics of novel *Coriolus versicolor* and *Lentinus edodes* kombucha beverages and immunomodulatory potential of their polysaccharide extracts. *Food Chemistry* 342:128344
30. Castillo JJ, Galermo AG, Amicucci MJ, Nandita E, Couture G, et al. 2021. A multidimensional mass spectrometry-based workflow for *de novo* structural elucidation of oligosaccharides from polysaccharides. *Journal of the American Society for Mass Spectrometry* 32:2175–85
31. Chen L, Long R, Huang G, Huang H. 2020. Extraction and antioxidant activities *in vivo* of pumpkin polysaccharide. *Industrial Crops & Products* 146:112199
32. Lv Y, Yang X, Zhao Y, Ruan Y, Yang Y, et al. 2009. Separation and quantification of component monosaccharides of the tea polysaccharides from *Gynostemma pentaphyllum* by HPLC with indirect UV detection. *Food Chemistry* 112:742–46
33. Wang B, Han L, Liu J, Zhang J, Wang W, et al. 2022. *Lycium* genus polysaccharide: an overview of its extraction, structures, pharmacological activities and biological applications. *Separations* 9:197
34. Wang L, Bao J, Wang L, Zhang F, Li Y. 2006. One-pot synthesis and bioapplication of amine-functionalized magnetite nanoparticles and hollow nanospheres. *Chemistry – A European Journal* 12:6341–47
35. Yang Y, Zhao M, Liu Y, Fang Z, Li Q, et al. 2022. Separation and identification of an abundant trigalloylglucose from special tea genetic resources. *Beverage Plant Research* 2:11
36. Yan T, Tao Y, Wang X, Lv C, Miao G, et al. 2021. Preparation, characterization and evaluation of the antioxidant capacity and antitumor activity of myricetin microparticles formed by supercritical antisolvent technology. *The Journal of Supercritical Fluids* 175:105290
37. Yan T, Wang H, Song X, Yan T, Ding Y, et al. 2022. Fabrication of apigenin nanoparticles using antisolvent crystallization technology: a comparison of supercritical antisolvent, ultrasonic-assisted liquid antisolvent, and high-pressure homogenization technologies. *International Journal of Pharmaceutics* 624:121981
38. Zhao Z, Huangfu L, Dong L, Liu S. 2014. Functional groups and antioxidant activities of polysaccharides from five categories of tea. *Industrial Crops and Products* 58:31–35
39. Wang S, Ding Y, Wang H, Li W, Xu W, et al. 2022. Molecularly imprinted upconversion nanoparticles for active tumor targeting and microinvasive photothermal therapy. *Journal of Materials Science* 57:5177–97
40. Zhou Y, Zhou X, Hong T, Qi W, Zhang K, et al. 2021. Lysosome-mediated mitochondrial apoptosis induced by tea polysaccharides promotes colon cancer cell death. *Food & Function* 12:10524–37
41. Zhang X, Yu H, Cai Y, Ke M. 2017. *Lycium barbarum* polysaccharides inhibit proliferation and migration of bladder cancer cell lines BIU87 by suppressing PI3K/AKT pathway. *Oncotarget* 8:5936–42
42. Liu X, Liu F, Zhao S, Guo B, Ling P, et al. 2019. Purification of an acidic polysaccharide from *Suaeda salsa* plant and its anti-tumor activity by activating mitochondrial pathway in MCF-7 cells. *Carbohydrate Polymers* 215:99–107
43. Cheng L, Chen L, Yang Q, Wang Y, Wei X. 2018. Antitumor activity of Se-containing tea polysaccharides against sarcoma 180 and comparison with regular tea polysaccharides and Se-yeast. *International Journal of Biological Macromolecules* 120:853–58



Copyright: © 2023 by the author(s). Published by Maximum Academic Press, Fayetteville, GA. This article is an open access article distributed under Creative Commons Attribution License (CC BY 4.0), visit <https://creativecommons.org/licenses/by/4.0/>.